Electronic Supplementary Material (ESI) for Dalton Transactions.

SUPPORTING INFORMATION

Bipyrrolidine salan alkoxide complexes of lanthanides: synthesis, characterisation, activity in the polymerisation of lactide and mechanistic investigation by DOSY NMR

James O. Beament, Gabriele Kociok-Köhn, Matthew D. Jones and Antoine. Buchard

Department of Chemistry, University of Bath, Claverton Down, Bath, BA2 7AY, UK

Email: mj205@bath.ac.uk (MDJ) ; a.buchard@bath.ac.uk (AB)

Contents

Experimental section

General Considerations

The preparation and characterisation of all metal complexes was carried out under an inert argon atmosphere using standard Schlenk or glovebox techniques. All chemicals used were purchased from Strem, Alfa Aesar and Sigma-Aldrich and used as received. Exceptions include *rac*-LA which was recrystallised twice from dry toluene and stored under glovebox conditions. Dry solvents used in handling metal complexes were obtained *via* SPS (solvent purification system) and dried over 3Å molecular sieves. $CDCl_3$ was dried over CaH_2 and distilled prior to use.

NMR Spectroscopy

^{1}H and homonuclear-decoupled ^{1}H NMR spectra of polymerisations were recorded on a Bruker 400 MHz instrument and referenced to residual solvent peaks. Coupling constants are given in Hertz. Polymerisation conversion was determined from the integration of the methine region of the polymer (5.12 - 5.20 ppm) against that of the monomer (4.94 – 5.01). The tacticity of polymers was determined from its homonuclear-decoupled ^{1}H NMR spectrum, decoupling at from the polymer doublet at 1.62 ppm. All ^{1}H, ^{13}C{^{1}H}, COSY and ^{1}H DOSY NMR experiments of lanthanide complexes and in-situ polymerisations were recorded on a Bruker Avance III 500 MHz spectrometer at concentrations of 10 mgmL^{-1}. The spectral width was expanded to encompass all notable signals. For DOSY polymerisation experiments each NMR tube was filled with 10 mg mL^{-1} of *rac*-LA in 1 mL deuterated $CDCl_3$. NMR samples were equilibrated at the measurement temperature of 25 °C for 5 min before data collection. Spinning was deactivated to avoid convection. 1D ^{1}H spectra were acquired with the zg30 pulse program from the Bruker library. 2D DOSY spectra were acquired using a double stimulated echo sequence ("dstegp2s") for convection compensation and with monopolar gradient pulses. Diffusion delay of 5 seconds, 64k data points and 32 scans per gradient level was used. Ten gradient strengths were used between 2 and 95 %. The spectra were multiplied with an exponential window function before Fourier transformation (xf2) and subsequently phase corrected. The diffusion coefficients were obtained on MestReNova processing software by fitting a peak heights fit method to the spectra. Diffusion constants are reported alongside the solvent diffusion signals and compared to those recorded in the literature.[1] Molecular weight estimations are made from use of the GNAT (V1.1.1) toolbox developed by Morris and coworkers, using an adapted stokes-einstein equations with a hard sphere approximation.[2,3]

Gel Permeation Chromatography

All polymers were characterised by a combination of gel permeation chromatography (GPC) and homo-nuclear decoupled ^{1}H NMR spectroscopy. GPC was carried out on a Agilent 1260 Infinity series instrument at 1 mLmin^{-1} at 35 °C with a THF eluent using a PLgel 5 μm MIXED-D 300 × 7.5 mm column. Detection was carried out using triple detection methods, using a differential refractive index detector (referenced to 11 polystyrene standards of narrow molecular weight, ranging from M_w 615-568000 Da), a viscometer detector and a light scattering detector (90°, with a calculated dn/dc range = 0.095-0.11 g^{-1}mL, as calculated from the RI). Multi analysis software was used to process the data.

MALDI-ToF Mass Spectrometry

MALDI-ToF analysis was carried out on a Bruker Autoflex speed instrument in reflector positive mode, using DCTB as the matrix at a concentration of 10 mg mL^{-1}. 50 μL of this solution was co-applied with 2 μL of 0.1 M NaTFA solution and 10 μL of the analyte at a concentration of 10 mg mL^{-1}. 1 μL of this homogenised solution was applied to a steel target plate for analysis. Materials characterisation (GPC, MALDI-ToF) facilities were provided through the Chemical Characterisation and Analysis Facility (CCAF) at the University of Bath.

Elemental Analysis

CHN microanalysis of all novel complexes was performed by Mr. Stephen Boyer at London Metropolitan University.

X-ray crystallography

All data were collected, at 150 K, on a Rigaku SuperNova diffractometer using radiation CuKα (λ= 1.54184 Å). Structures were solved by direct methods throughout and refined on F^2 data using the SHELXL-2014 suite of programs. All hydrogen atoms were included in idealised positions and refined using the riding model. Refinements were straightforward with only the following points that merit note: [{L^{Me}Yb(O*i*Pr)}$_2$] The crystal was Twinned about the 0.6, 0, -0.8 axis by ca. 8%. One molecule of toluene was present in the asymmetric unit cell – given the disorder the H-atoms could not be located and are consequently removed from the model but are left in the formula. [$L^{tBu}{}_2Yb_2$(O*i*Pr)(OH)] two t-Bu groups of the complex show rotational disorder in the ratio 70:30 (C11-C14/C11A-C14A) and 56:44 (C67, C68, C72-C75/C67A, C68A, C72A-C75A). Atom C12 has been refined with ADP restraints. All solvent molecules are disordered over two sites in the ratio 1:1. One hexane molecule (C81-C86) is located close to a centre of inversion and was refined with bond lengths restraints and 50% occupation. One toluene molecule (C101-C107) is disordered over a centre of inversion and was refined with 50% occupation. The other toluene molecule (C91-C97/C91A-C97A) was refined with ADP restraints [{L^{tBu}Nd(O*i*Pr)}$_2$] The crystal was twinned ca. 26% about the 0, 0, 1. Two molecules of toluene were present in the asymmetric unit, one was modelled over two sites in a 55:45 ratio and restraints were necessary to afford reasonable ADP. [{L^{Me}Sm(O*i*Pr)}$_2$] the solvent molecule of toluene is disordered and lying close to a centre of inversion therefore was refined with 50% occupation. All toluene atoms were refined with geometric constraints and additionally with ADP restraints. [{L^{tBu}Sm(OH)}$_2$] the asymmetric unit consists of half a dimeric Sm complex and 1.5 molecules of toluene. One t-Bu group (C13, C14) of the complex ligand shows disorder over two sites in the ratio 2:1. The minor part atoms were refined with ADP restraints necessary to aid convergence. One toluene is disordered over two sites in the ratio 2:1 and the other is lying on a centre of inversion and was refined with 50% occupation. [(L^{tBu})$_2$Sm$_2$(O*i*Pr)(OH)] no specific comments. [{L^{tBu}Sm(O*i*Pr)}$_2$] One t-Bu group of the complex ligand shows disorder over two sites in the ratio 60:40 (C38-C41) and another in 50:50 ratio (C15-C17). One molecule of hexane was present in the unit cell and this was disordered over two sites in a 60:40 ratio and restraints were necessary to aid convergence.

Synthetic Protocols

Synthesis of Ln complexes

The preparation of ligands $L^{Me}H_2$ and $L^{tBu}H_2$ were carried out following literature procedures.[4] In a typical experiment: $L^{tBu}H_2$ (576 mg, 1.0 mmol) was dissolved in toluene (5 mL) was added to a stirred solution of $Nd(O^iPr)_3$ (1.0 mmol) in toluene (10 mL). The solution was then heated to 60 °C and left to stir for 3 hours. After this time the solvent was removed and the solid was dissolved in the minimum quantity of dry hexane/toluene and left to recrystallise at -20 °C. The crystalline material was washed with cold hexane (3 x 1 mL) and dried under a vacuum. Where possible ^{1}H NMR and $^{13}C\{^1H\}$ NMR and ^{1}H DOSY spectra were collected for analysis. Otherwise each single crystal XRD and CHN microanalysis was used for characterisation.

Hydrolysis reactions were carried out by exposing a J-Youngs tube solution of lanthanide sample in $CDCl_3$ to a flow of compressed air through the solution via a needle for 30 mins. The vessel was sealed and monitored via ^{1}H NMR spectroscopy.

[{L^{Me}Sm(O*i*Pr)}$_2$]. White powder (310 mg, 51% yield). ^{1}H NMR (500 MHz, $CDCl_3$, δ_H, ppm); 7.92 (2H, Ar*H*), 7.43 (2H, Ar*H*), 6.90 (2H, Ar*H*), 6.25 (2H, d, J = 12.5 Hz, C*H*H), 6.18 (2H, OC*H*$(CH_3)_2$), *6*.01 (6H, C*H*$_3$), 5.21 (2H, C*H*H), 4.8 (2H, Ar*H*), 2.83 (2H, d, J = 12.5 Hz, CH*H*), 2.50 (6H, C*H*$_3$), 2.05 - 2.32 (12H, OCH(C*H*$_3)_2$), 2.00 (6H, C*H*$_3$), 1.88 (2H, CH*H*), 0.72 (4H, C*H*$_2$), 0.2 (6H, C*H*$_3$), -0.04 (2H, C*H*), -0.33 (2H, C*H*), -0.33 (2H, C*H*), -0.69 (4H, C*H*$_2$), -1.02 (4H, C*H*$_2$), -1.53 (2H, C*H*), -2.45 (2H, C*H*), -2.70 (2H, C*H*), -4.07 (2H, C*H*), -4.56 (2H, C*H*). 2D DOSY (500 MHz, $CDCl_3$ D_{sol}= 1.77x10^{-9} m^{2}s^{-1}, 298 K,) 5.89 x10^{-10} m^{2}s^{-1}. Elemental (CHN) Analysis; (Calculated: $C_{58}H_{82}N_4O_6Sm_2$) C: 56.54%, H: 6.71%, N: 4.55%, (Experimental) C: 56.70%, H: 6.81%, N: 4.46%.

[{L^{Me}Yb(O*i*Pr)}$_2$]. White powder (298 mg, 47% yield). Elemental (CHN) Analysis; (Calculated: $C_{58}H_{82}N_4O_6Yb_2$) C: 54.53%, H: 6.47%, N: 4.39%, (Experimental) C: 54.16%, H: 6.59%, N: 4.34%.

[{L^{tBu}Sm(O*i*Pr)}$_2$]. White powder (55 mg, 7% yield). (Elemental (CHN) Analysis; (Calculated: $C_{82}H_{130}N_4O_6Sm_2$) C: 62.79%, H: 8.35%, N: 3.57%, (Experimental) C: 63.41%, H: 8.79%, N: 3.61%.

[{L^{tBu}Nd(O*i*Pr)}$_2$]. Blue powder (680 mg, 86% yield). Elemental (CHN) Analysis; (Calculated: $C_{82}H_{130}N_4O_6Nd_2$) C 63.2 %, H: 8.42%, N: 3.60%, (Experimental) C: 62.74%, H: 8.16%, N: 3.62%.

[L^{tBu}_2Sm$_2$(O*i*Pr)(OH)]. Cream powder (530 mg, 69% yield) (Elemental (CHN) Analysis; (Calculated: $C_{79}H_{124}N_4O_6Sm_2$) C: 62.16%, H: 8.19%, N: 3.67%, (Experimental) C: 61.66%, H: 8.15%, N: 3.68%.

[L^{tBu}_2Yb$_2$(O*i*Pr)(OH)]. White powder (180 mg, 23% yield). Elemental (CHN) Analysis; (Calculated: $C_{79}H_{124}N_4O_6Yb_2$) C: 60.36%, H: 7.95%, N: 3.56%, (Experimental) C: 59.72%, H: 7.64%, N: 3.57%.

[{L^{tBu}Sm(OH)}$_2$]. White powder (90 mg, 17.5% yield) ^{1}H NMR (500 MHz, $CDCl_3$, δ_H, ppm); 22.36 (1H, SmO*H*), 8.28 (2H, Ar*H*), 8.05 (2H, Ar*H*), 6.63 (2H, CH*H*), 3.14 (4H, NC*H*$_2$), 2.87 (2H, C*H*H), 1.93 (18H, (C(C*H*$_3)_3$)), 0.54 (18H, (C(C*H*$_3)_3$)), -0.85 (2H, C*H*$_2$), -2.04 (2H, C*H*$_2$), -3.02 (2H, C*H*$_2$), -4.48 (2H, C*H*$_2$), -7.22 (2H, C*H*$_2$); $^{13}C\{^1H\}$ NMR (100 MHz, $CDCl_3$, δ_C, ppm); 172.4 (*C*-O), 137.1 (Ar), 135.7 (Ar), 128.4 (Ar), 127.8 (Ar), 126.0 (Ar), 66.6 (N*C*H), 59.6 (N*C*H$_2$), 52.8 (N*C*H$_2$), 36.0 (*C*(CH$_3)_3$), 35.2 (*C*(CH$_3)_3$), 32.6 (*C*(*C*H$_3)_3$), 29.6 (C(*C*H$_3)_3$), 22.8 (*C*H)$_2$, 18.7 (*C*H)$_2$, 16.8 (*C*H)$_2$, 14.3 (*C*H)$_2$. 2D DOSY (500 MHz, $CDCl_3$, D_{sol}= 2.09x10^{-9} m^{2}s^{-1}, 298 K,) 4.69 x10^{-10} m^{2}s^{-1}. Elemental (CHN) Analysis,

(Calculated: $C_{76}H_{118}N_4O_6Sm_2$) C: 61.49 %, H: 8.01 %, N 3.77 %, (Experimental) C: 60.96 %, H 7.77 %, N 3.74 %.

Polymerisation of *rac*-lactide

Typical polymerisation procedure (Solution): *rac*-lactide (1.0 g, 6.9 $x10^{-3}$ mol) was added to an ampule with a Young's cap in 10 mL of solvent, with initiator (6.9 $x10^{-6}$ mol). If toluene was the chosen solvent, the polymerisation ran at 80 °C for the chosen time, whereas polymerisations in CH_2Cl_2 were carried out at 25 °C. Once complete the solvent was immediately removed *in vacuo* and the crude product analysed via ^{1}H NMR.

Typical polymerisation procedure (*in-situ* kinetics): *rac*-lactide (60 mg, 4.16 $x10^{-4}$ mol) was added to an NMR ampule with a Young's cap in 0.6 mL of tol-d_8, with initiator (1.38 $x10^{-6}$ mol). The vessel was allowed to equilibrate at 80 °C for 5 minutes, the magnetic field was homogenised and experiments were ran with 5 minutes intervals until completion. Polymerisations tracked by DOSY were carried out at concentrations of 10 $mgmL^{-1}$ of *rac*-LA using a premade stock solution of the chosen initiator. Quenching of the vessel was carried out by bubbling compressed air through the tube for 5 minutes.

Typical polymerisation procedure (Melt): *rac*-lactide (1.0 g, 6.9 $x10^{-3}$ mol) was added to an ampule with a Young's cap with initiator (7.7 $x10^{-6}$ mol) and placed into an oil bath set at 130 °C. Upon reaching the gel point the vial was exposed to air and approximately 5 mL of reagent grade CH_2Cl_2 was added quench the polymerisation. Removal of the solvent *in vacuo* yielded the crude product which was analysed via ^{1}H NMR spectroscopy. The polymer was then washed with methanol (3 x 10 mL) and dried under high vacuum.

^{1}H, ^{13}C{^{1}H} and ^{1}H DOSY NMR spectra of lanthanide complexes

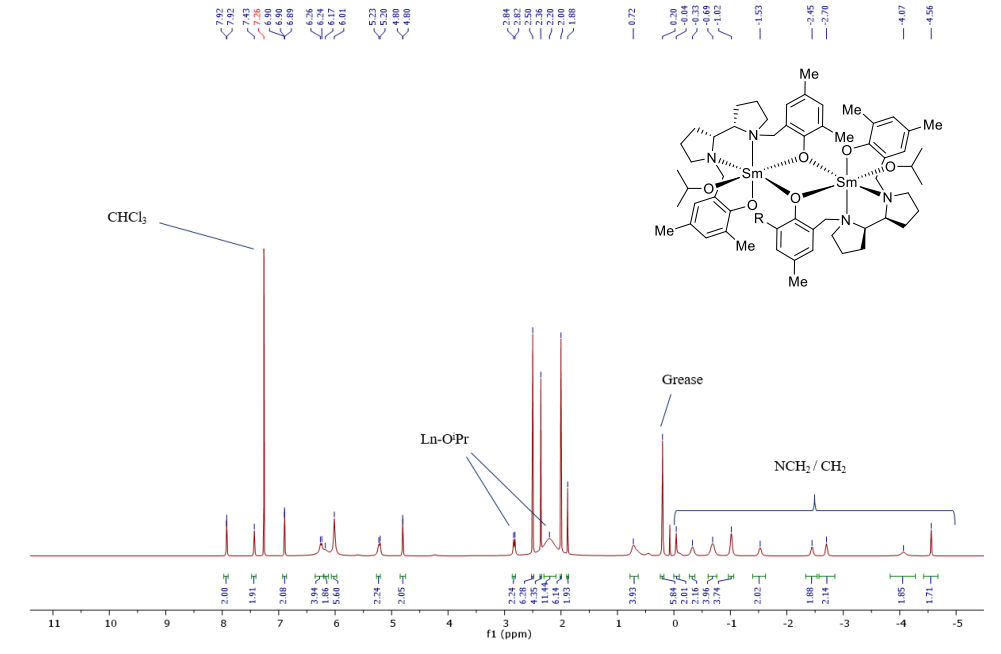

Figure S1. ^{1}H NMR spectra of [{L^{Me}Sm(O*i*Pr)}$_2$] in $CDCl_3$.

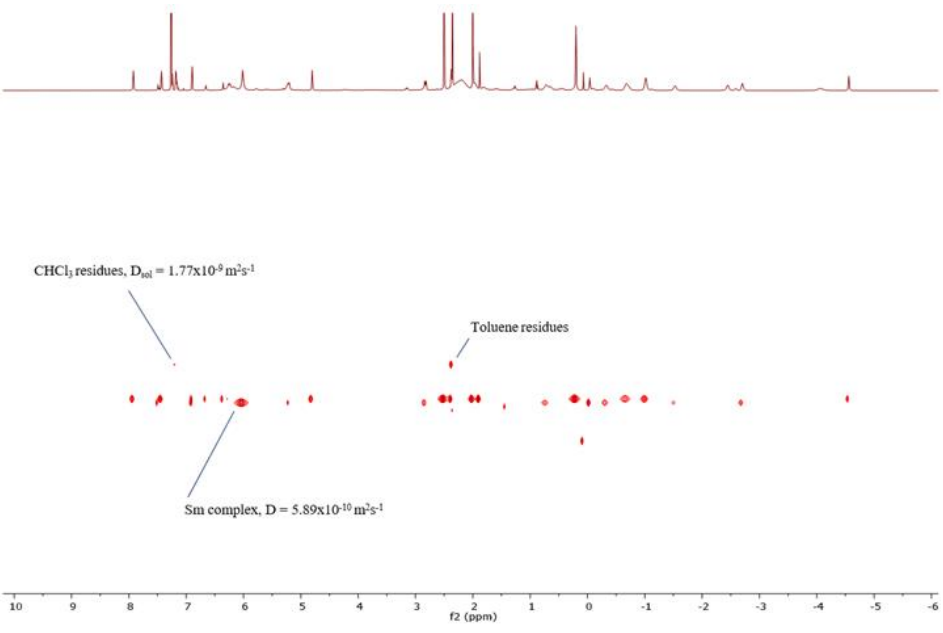

Figure S2. ^{1}H DOSY NMR spectra of [{L^{Me}Sm(O*i*Pr)}$_2$] in $CDCl_3$ at 25 °C.

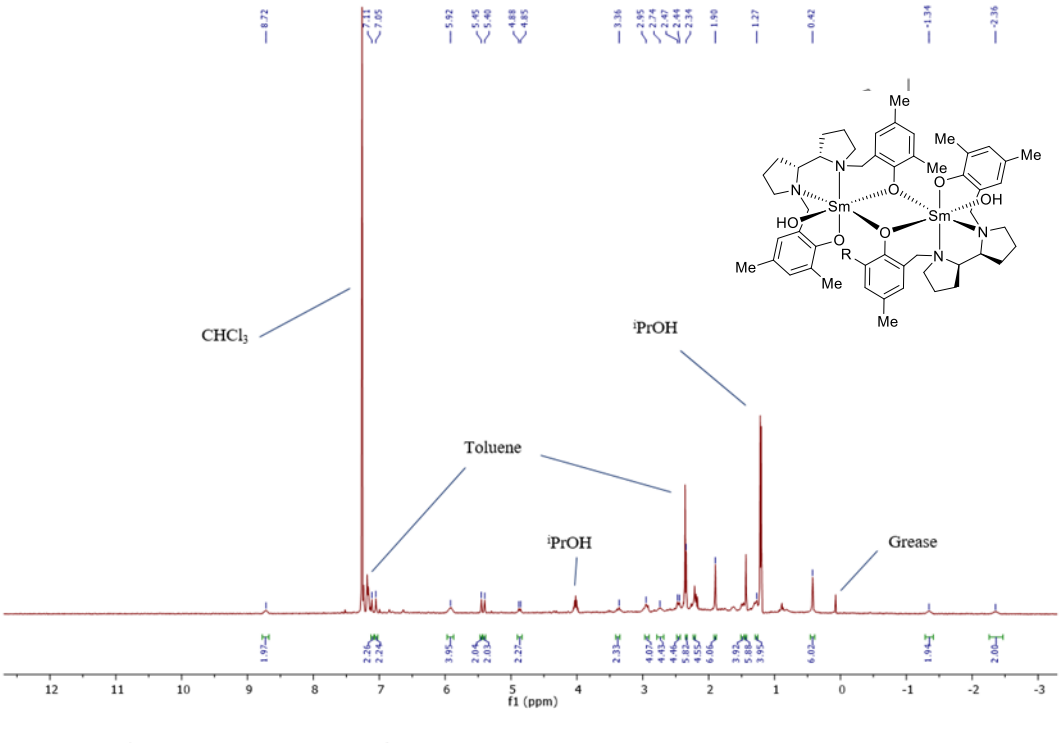

Figure S3. ^{1}H NMR of hydrolysed [{L^{Me}Sm(O*i*Pr)}$_2$] species $CDCl_3$ at 298 K. The presence of free *i*PrOH and complex signals leads to the postulation of a di-OH hydrolysis product, [{L^{Me}Sm(OH)}$_2$].

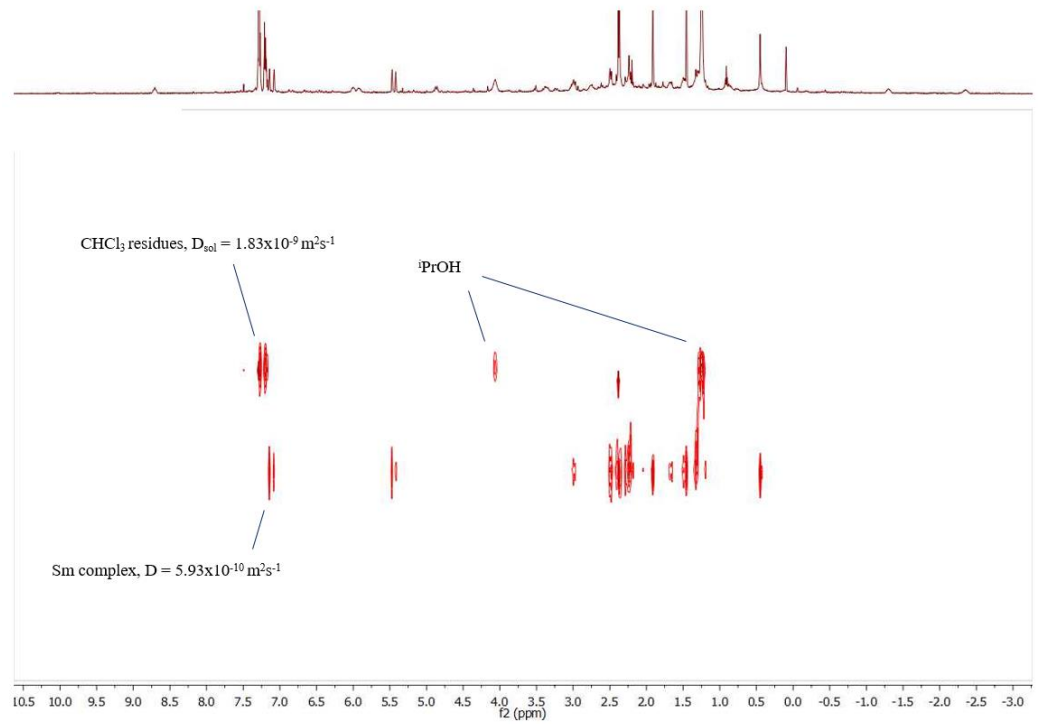

Figure S4. ^{1}H DOSY NMR spectra of [{L^{Me}Sm(OH)}$_2$] in $CDCl_3$ at 25 °C. Presence of free *i*PrOH is evidenced by a faster diffusion signal for the *i*PrOH species than the Sm species.

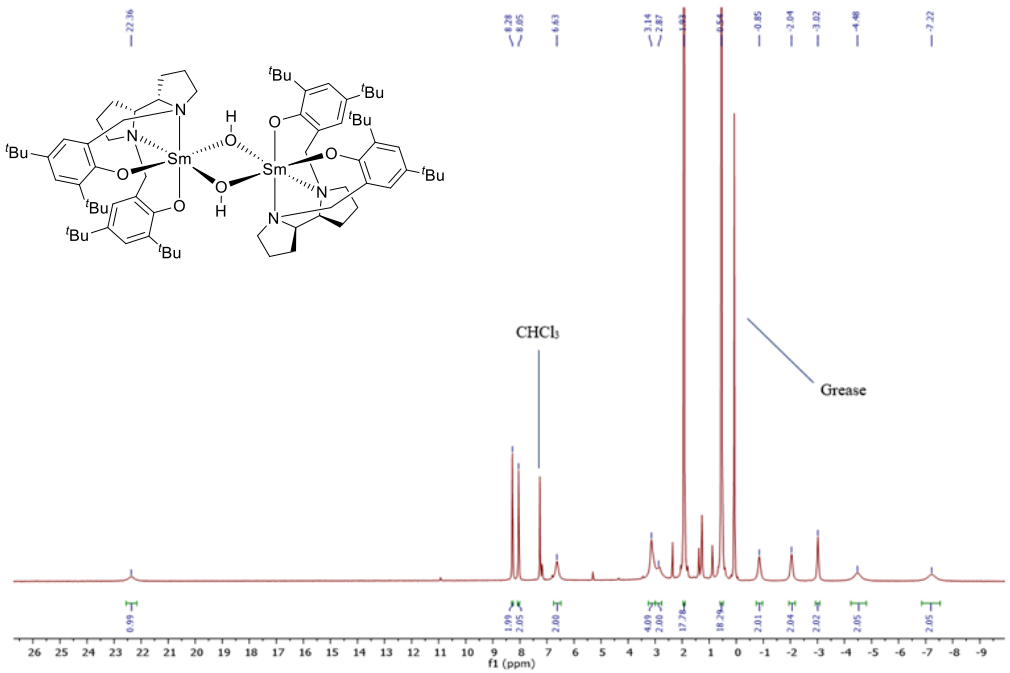

Figure S5. ^{1}H NMR spectra of [{L$^{t\text{Bu}}$Sm(OH)}$_2$] in $CDCl_3$.

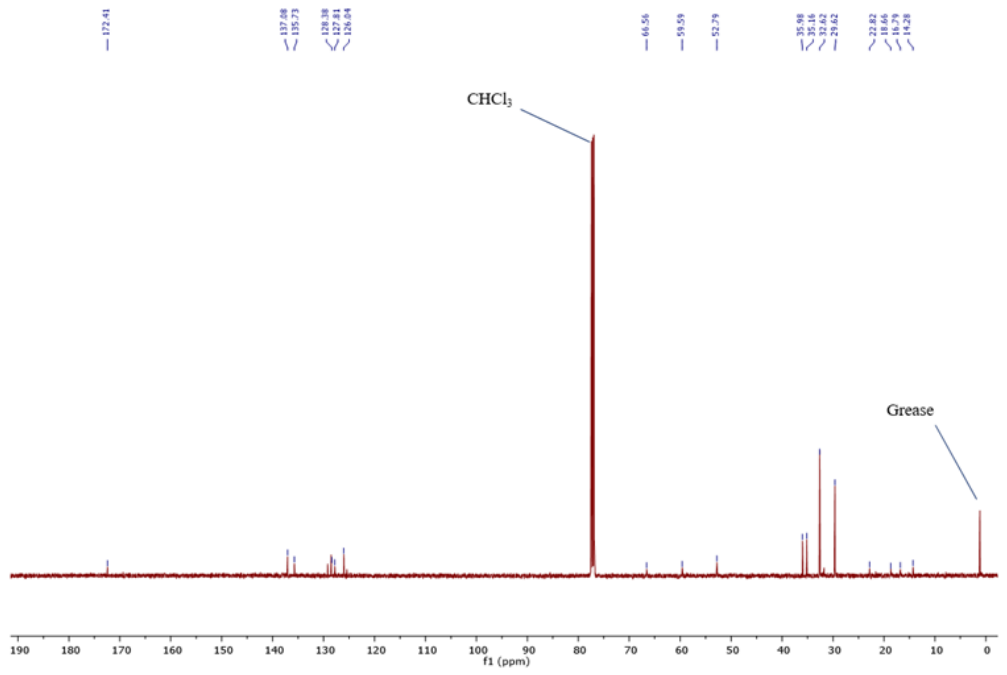

Figure S6. ^{13}C{^{1}H} NMR spectra of [{L$^{t\text{Bu}}$Sm(OH)}$_2$] in $CDCl_3$ at 25 °C.

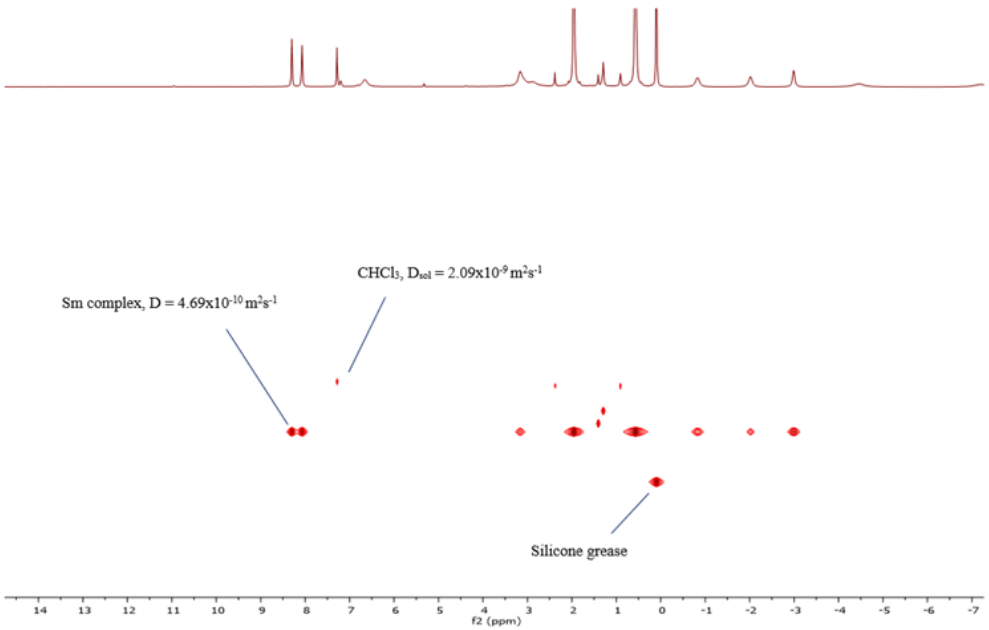

Figure S7. ^{1}H DOSY NMR spectra of [{L$^{t\mathrm{Bu}}$Sm(OH)}$_2$] in $CDCl_3$ at 25 °C.

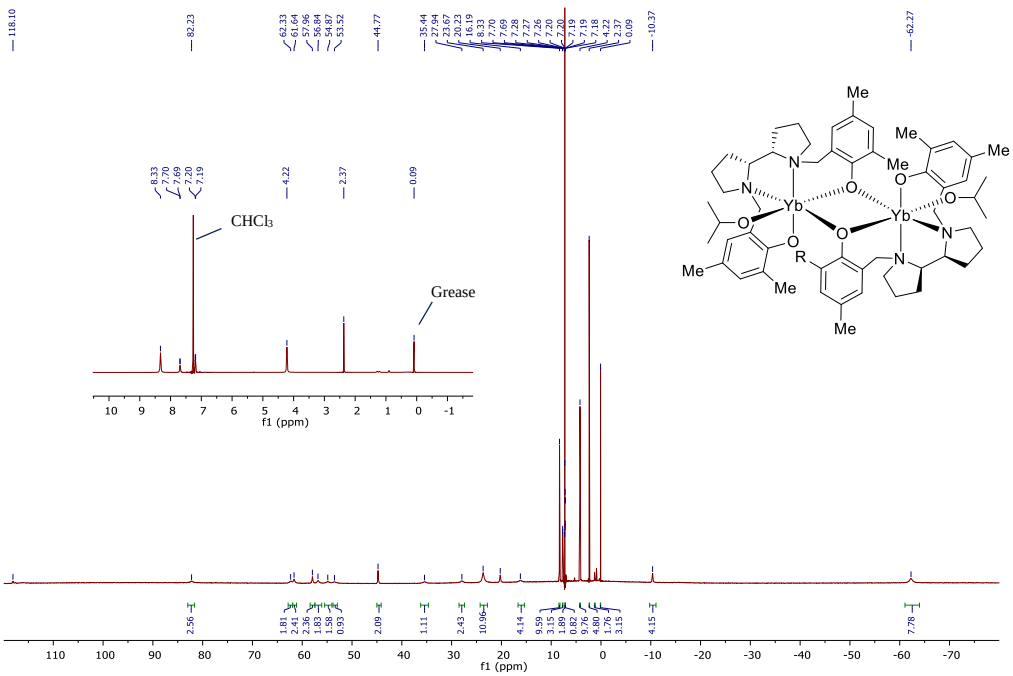

Figure S8. ^{1}H NMR spectra of [{L$^{\mathrm{Me}}$Yb(O*i*Pr)}$_2$] in $CDCl_3$ at 25 °C. Large spectral width and significant line broadening meant full characterisation was not possible.

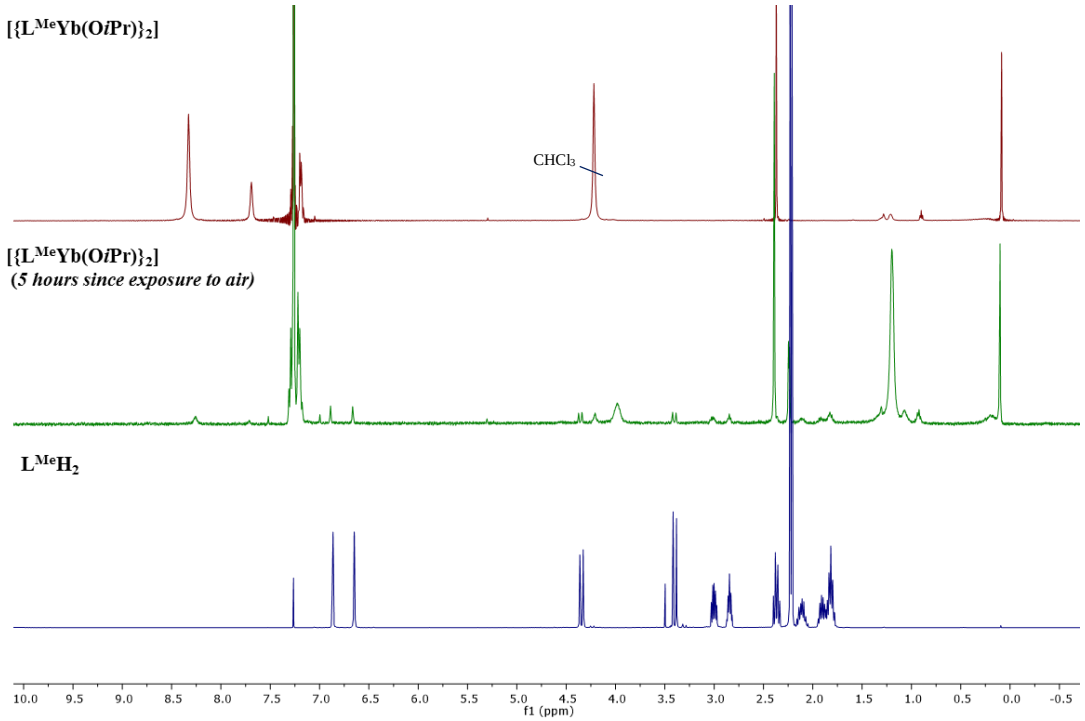

Figure S9. Stacked ^{1}H NMR spectra of the hydrolytic degradation of [{L^{Me}Yb(O*i*Pr)}$_2$] upon exposure to air, 25 °C, $CDCl_3$. Similarities to the free ligand suggest complete degradation of the complex after this time frame. Evidence of free iso-propanol suggests the Yb species is likely a hydroxide product.

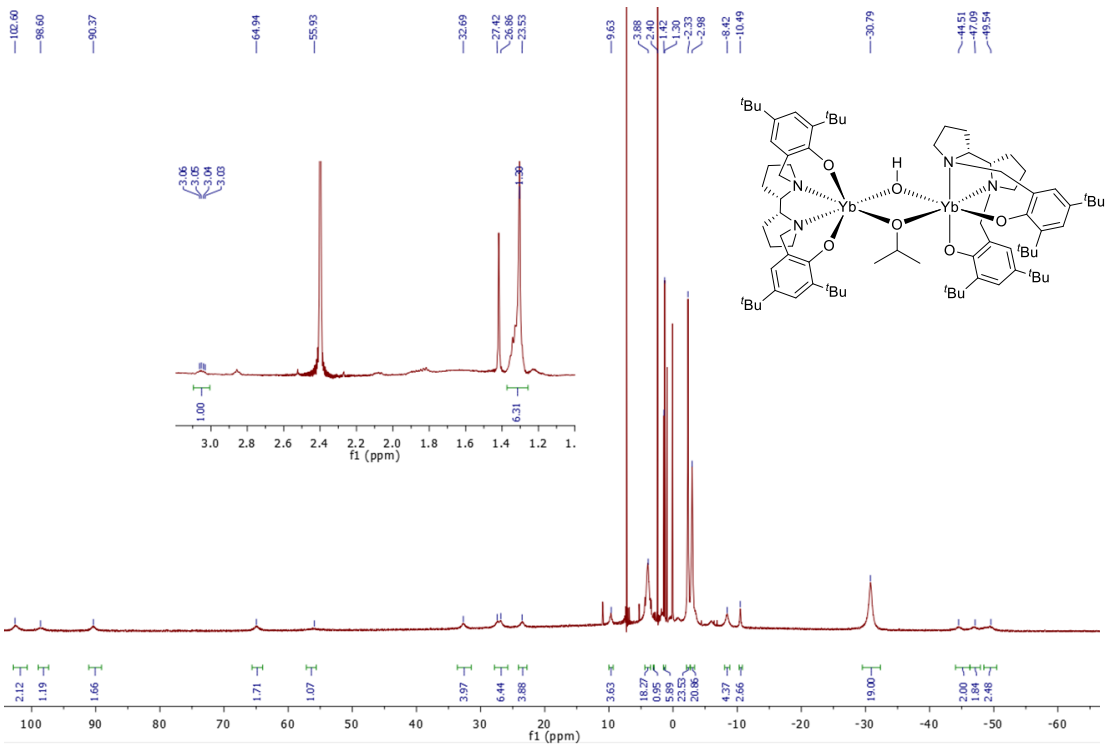

Figure S10. ^{1}H NMR spectra of [L$^{tBu}{}_2$Yb$_2$(O*i*Pr)(OH)] in $CDCl_3$ at 25 °C. Large spectral width and significant line broadening meant full characterisation was not possible. However, It is possible to identify the mono-alkoxide (3.05 and 1.30 ppm) and signals corresponding to ^{t}Bu groups (3.88, -2.33, -2.98 and -30.79 ppm).

In-situ DOSY polymerisation studies using [{L^{Me}Sm(O*i*Pr)}$_2$]

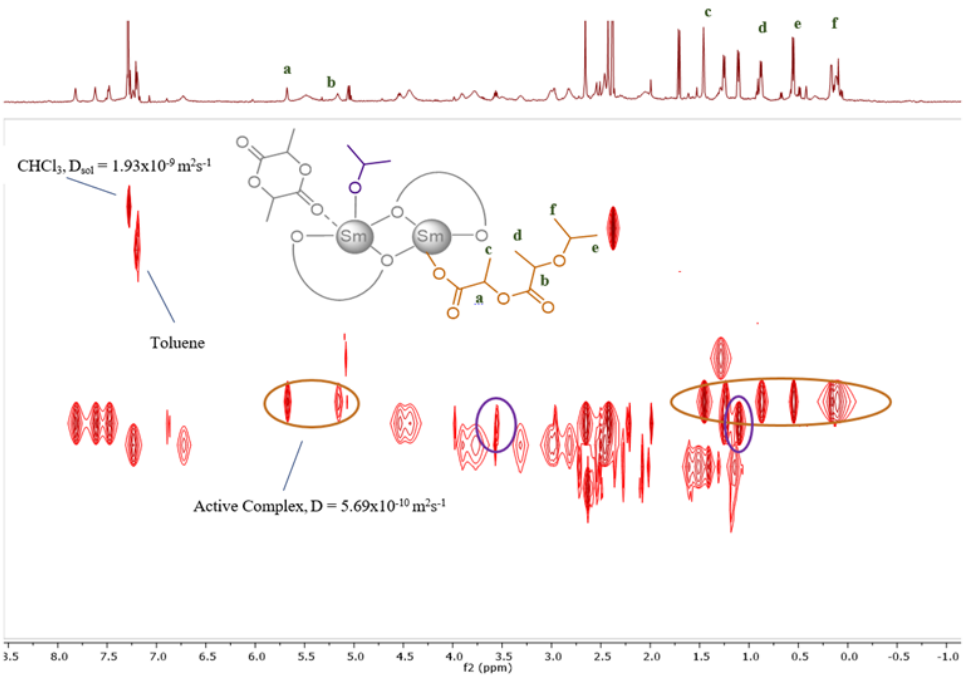

Figure S11. ^{1}H DOSY NMR of a polymerisation of rac-LA initiated with [{L^{Me}Sm(O*i*Pr)}$_2$] at a 2:1 ratio {[LA]:[Ln]}, [LA] = 0.069 M, 25 °C, 5 hours, $CDCl_3$.

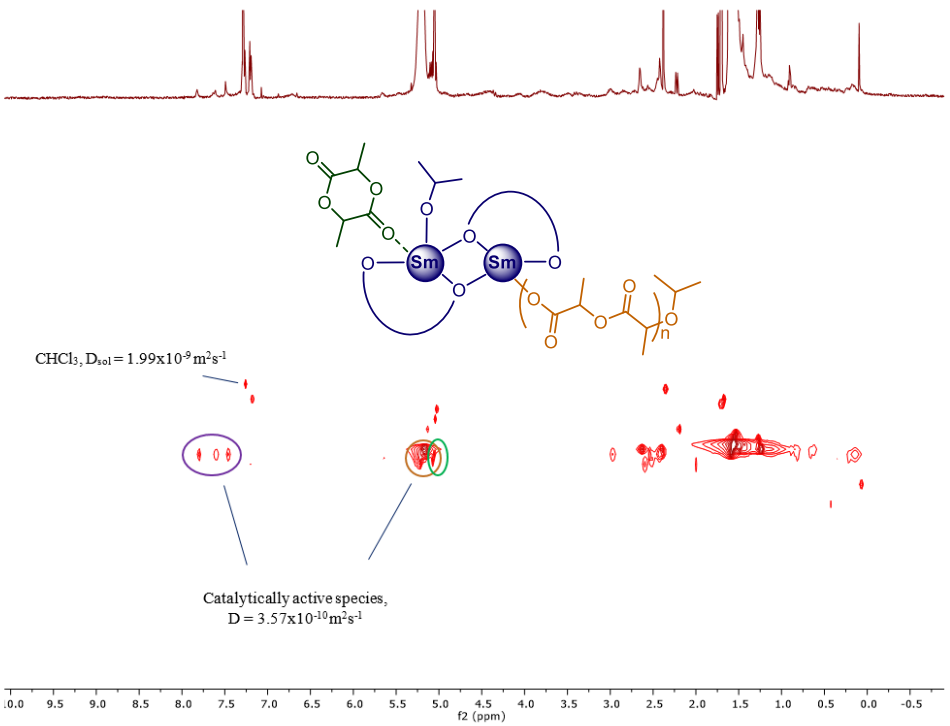

Figure S12. ^{1}H DOSY NMR of a polymerisation of rac-LA initiated with [{L^{Me}Sm(O*i*Pr)}$_2$] at a 20:1 ratio {[LA]:[Ln]}, [LA] = 0.069 M, 25 °C, 5 hours, $CDCl_3$ (Entry 2, Table 5).

Polymerisation data

Table S1. Selected polymerisation data for the polymerisation of *rac*-lactide. [LA] = 0.69 M, solvent = CH_2Cl_2, T = 25 °C.

Entry	Initiator	Ratio [LA]:[Ln][a]	Time (min)	Con.[b] %	*Theor.* M_n[c] kgmol^{-1}	M_n[d] kgmol^{-1}	$Đ$ [d]	P_r [e]
1	[{L^{tBu}Nd(O*i*Pr)}$_2$]	500	60	96	68.5	117.2	1.38	0.6
2	[{L^{tBu}Nd(O*i*Pr)}$_2$]	1000	60	95	136.9	247.2	1.05	0.61
3	[{L^{Me}Sm(O*i*Pr)}$_2$]	150	120	40	8.7	5.8	1.03	0.58
4	[{L^{Me}Sm(O*i*Pr)}$_2$]	1000	120	5	-	-	-	-
5	[{L^{Me}Yb(O*i*Pr)}$_2$]	500	120	3	-	-	-	-
6	[L$^{tBu}_2$Sm$_2$(O*i*Pr)(OH)]	300	120	95	41.1	41.9	1.51	0.6
7	[L$^{tBu}_2$Sm$_2$(O*i*Pr)(OH)]	1000	120	95	136.9	92.9	1.51	0.59
8	[L$^{tBu}_2$Yb$_2$(O*i*Pr)(OH)]	500	120	39	28.8	36.5	1.05	0.71
9	[L$^{tBu}_2$Yb$_2$(O*i*Pr)(OH)]	1000	120	26	37.5	44.6	1.05	0.67

[a] Concentration of initiator based on per alkoxide initiating group. [b]Determined from analysis of the ^{1}H NMR spectrum by integration of the methine region (LA, 4.96 - 5.04 ppm; PLA, 5.10 - 5.22 ppm). [c]Theoretical M_n = (144.12 x Equiv LA) x (Conv/100) + MW of end groups (O^{i}Pr + H). [d] As Determined by GPC (THF) using triple detection methods. [e] As determined from ^{1}H{^{1}H} NMR from decoupling of the methine region using values predicted according to Bernoullian statistics.

Table S2. Selected polymerisation data for the polymerisation of *rac*-lactide. [LA] = 0.69 M, Solvent = toluene, T = 80 °C.

Entry	Initiator	Ratio [LA]:[Ln][a]	Time (min)	Con.[b] %	*Theor.* M_n[c] kgmol^{-1}	M_n[d] kgmol^{-1}	$Đ$ [d]
1	[{L^{tBu}Nd(O*i*Pr)}$_2$]	500	5	96	68.5	208.3	1.36
2	[{L^{tBu}Nd(O*i*Pr)}$_2$]	1500	5	95	205.3	156.3	1.30
3	[{L^{tBu}Nd(O*i*Pr)}$_2$]	3000	10	96	410.5	370.8	1.10
4	[{L^{Me}Sm(O*i*Pr)}$_2$]	500	5	96	69.1	350.0	1.36
5	[{L^{Me}Sm(O*i*Pr)}$_2$]	1500	10	96	207.4	169.4	1.23
6	[L$^{tBu}_2$Sm$_2$(O*i*Pr)(OH)]	1500	10	95	205.3	141.4	1.31
7	[{L^{tBu}Sm(OH)}$_2$]	1500	10	8	17.4	49.0	1.14
8	[{L^{Me}Yb(O*i*Pr)}$_2$]	1500	10	80	173.0	101.3	1.07
9	[L$^{tBu}_2$Yb$_2$(O*i*Pr)(OH)]	500	10	95	68.5	69.0	1.11

[a] Concentration of initiator based on per alkoxide initiating group. [b]Determined from analysis of the ^{1}H NMR spectrum by integration of the methine region (LA, 4.96 - 5.04 ppm; PLA, 5.10 - 5.22 ppm). [c]Theoretical M_n = (144.12 x Equiv LA) x (Conv/100) + MW of end groups (O^{i}Pr + H). [d] As Determined by GPC (THF) using triple detection methods.

Table S3. Selected polymerisation data for the polymerisation of *rac*-lactide. [LA] = 0.69 M, [LA]:[Ln] = 900:1, Solvent = N/A, T = 130 °C

Entry	Initiator	Time (min)	Con.[a] %	*Theor.* M_n[b] kgmol^{-1}	M_n[c] kgmol^{-1}	$Đ$ [c]
1	[{L^{tBu}Nd(O*i*Pr)}$_2$]	5	95	123.1	122.1	1.05
2	[{L^{Me}Sm(O*i*Pr)}$_2$]	5	74	96.0	136.4	1.45
3	[L$^{tBu}_2$Sm$_2$(O*i*Pr)(OH)]	5	82	106.4	136.4	1.45
4	[{L^{Me}Yb(O*i*Pr)}$_2$]	5	91	118.1	128.8	1.24
5	[L$^{tBu}_2$Yb$_2$(O*i*Pr)(OH)]	5	82	106.4	62.1	1.36

[a]Determined from analysis of the ^{1}H NMR spectrum by integration of the methine region (LA, 4.96 - 5.04 ppm; PLA, 5.10 - 5.22 ppm). [b]Theoretical M_n = (144.12 x Equiv LA) x (Conv/100) + MW of end groups (O^{i}Pr + H). [c]As Determined by GPC (THF) using triple detection methods.

Kinetic Studies

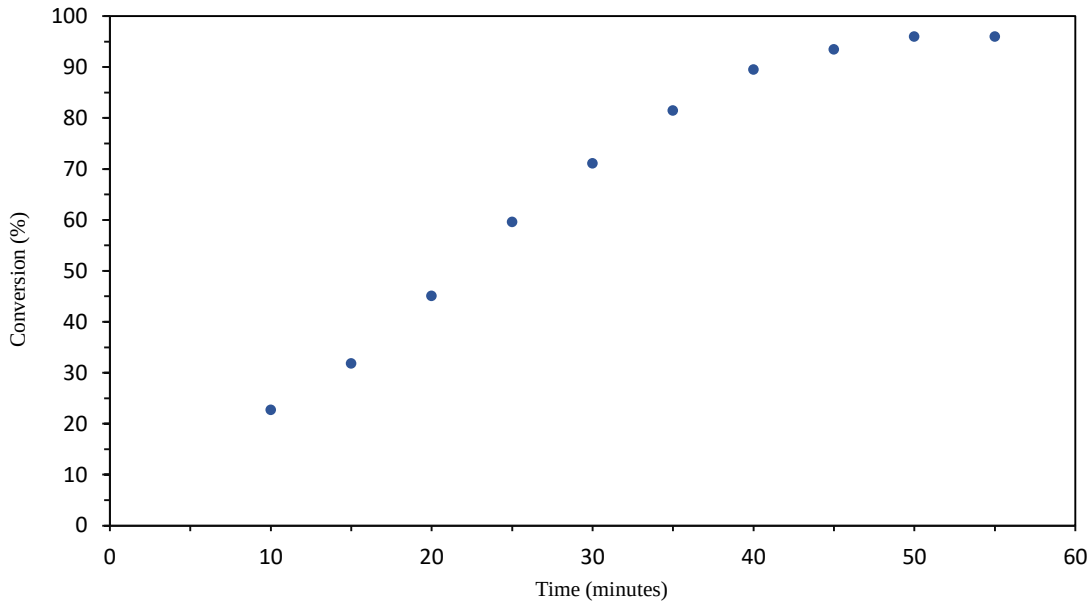

Figure S13. Plot of conversion vs time for the polymerisation of *rac*-lactide using [{L^{tBu}Nd(O*i*Pr)}$_2$] at 25 °C in $CDCl_3$. $[LA]_0$ = 0.69 M, ratios of 150:1 {[LA]:[Ln]}. Time samples taken via in-situ NMR experimentation.

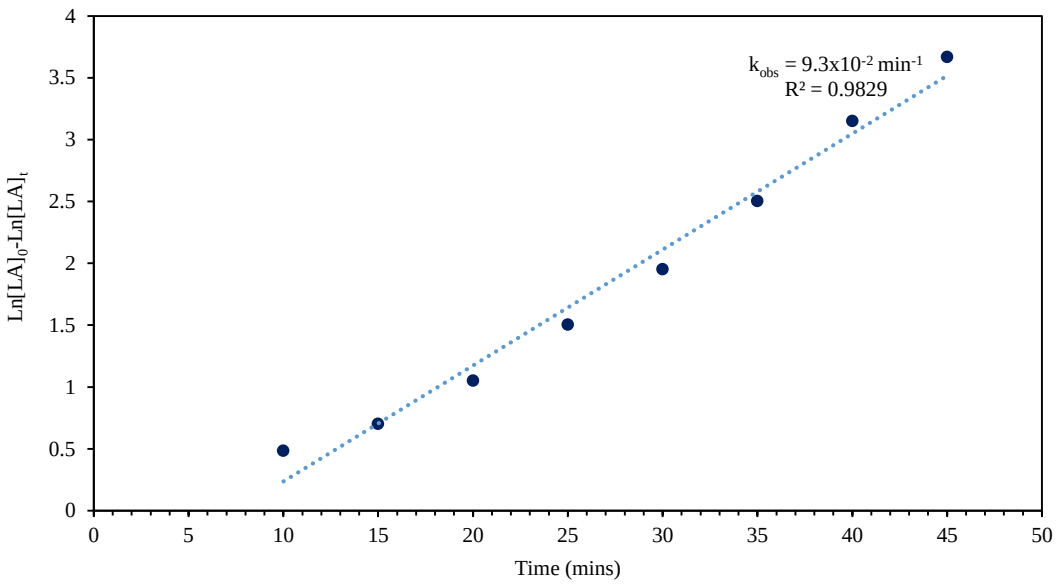

Figure S14. Linear plot of $Ln[LA]_0$-$Ln[LA]_t$ vs time for the polymerisation of *rac*-lactide using [{L^{tBu}Nd(O*i*Pr)}$_2$] at 25 °C in $CDCl_3$. $[LA]_0$ = 0.69 M, ratios of 150:1 {[LA]:[Ln]}.Time samples taken via in-situ NMR experimentation. The linear relationship shows the initial rate follows a pseudo-first order kinetic profile with a k_{obs} = 1.7x10^{-3} s^{-1}.

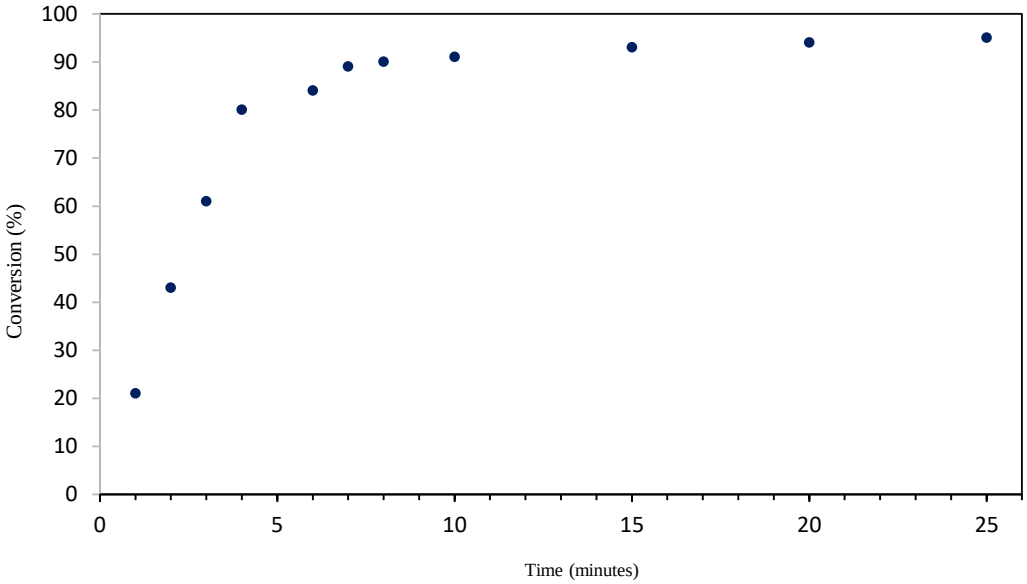

Figure S15. Plot of conversion vs time for the polymerisation of *rac*-lactide using [{L^{tBu}Nd(O*i*Pr)}$_2$] at 80 °C in toluene at ratios of 1500:1 {[LA]:[Ln]}. Time samples taken via aliquots from the stirred solution.

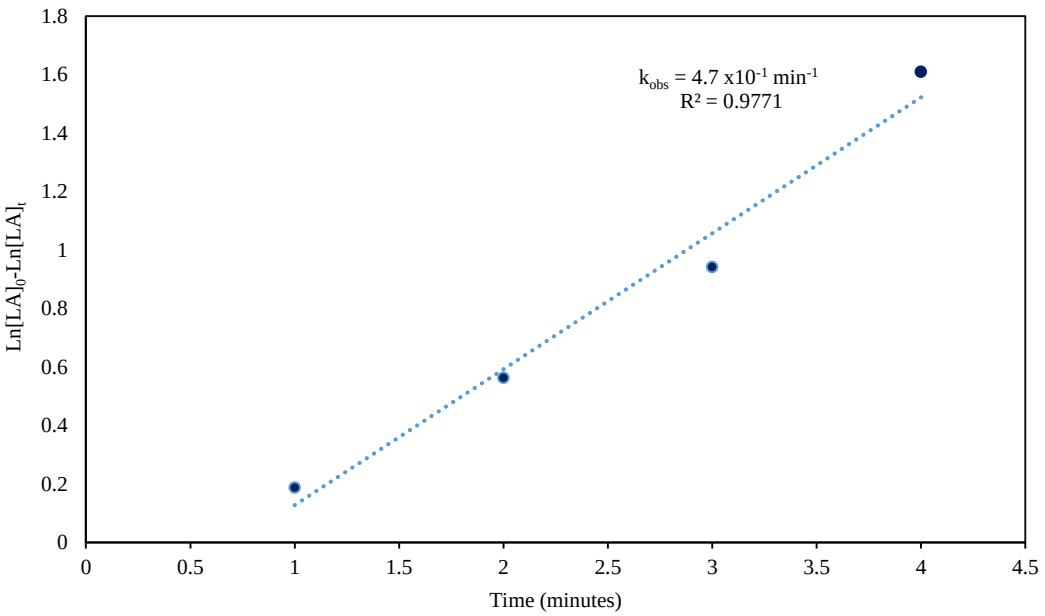

Figure S16. Linear plot of Ln[LA]$_0$-Ln[LA]$_t$ vs time for the polymerisation of *rac*-lactide using [{L^{tBu}Nd(O*i*Pr)}$_2$] at 80 °C in toluene at ratios of 1500:1 {[LA]:[Ln]}. Time samples taken via aliquots from the stirred solution. Plot shows the first 4 time sequences highlighting the initial rate. The linear relationship shows the initial rate follows a pseudo-first order kinetic profile.

a)

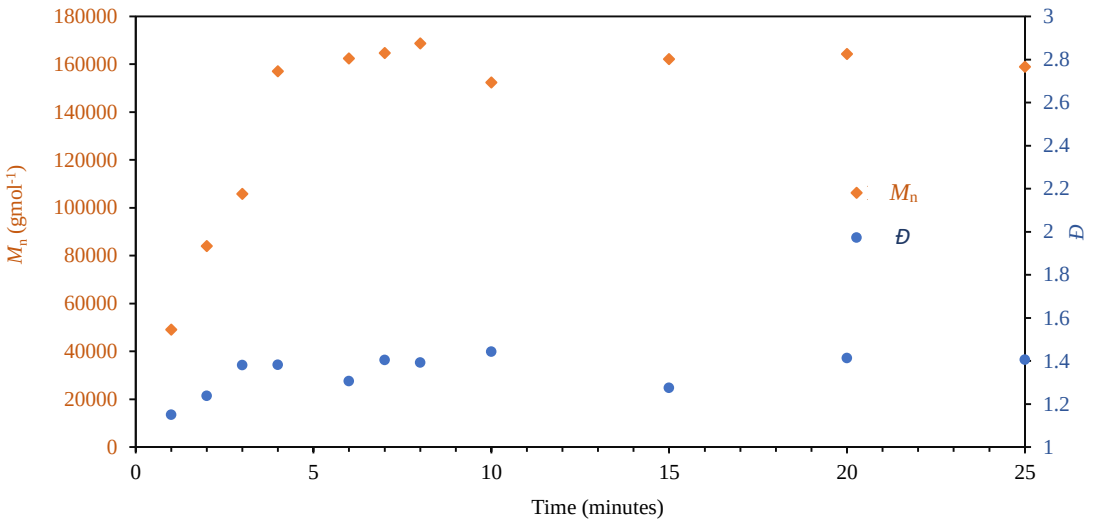

b)

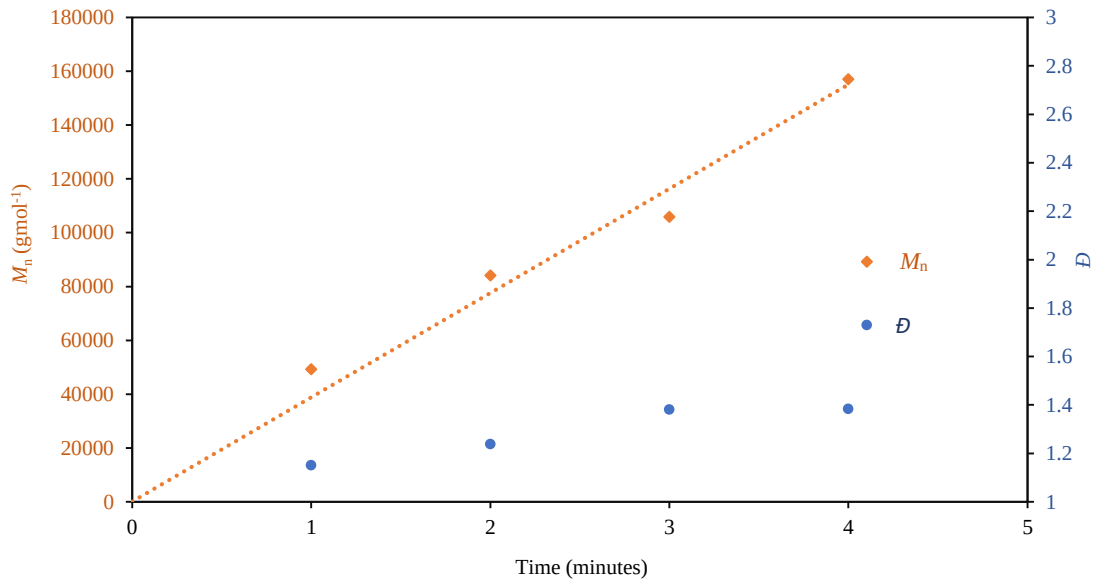

Figure S17. Plot of M_n vs time for the polymerisation of rac-lactide using [{L^{tBu}Nd(O*i*Pr)}$_2$] at 80 °C in toluene at ratios of 1500:1 {[LA]:[Ln]}. Time samples taken via the aliquots method. A) Shows the overall profile of M_n and poly dispersity ($Đ$) vs time for the reaction B) Shows the first 4 time sequences highlighting the linear growth of polymer chains at low conversion.

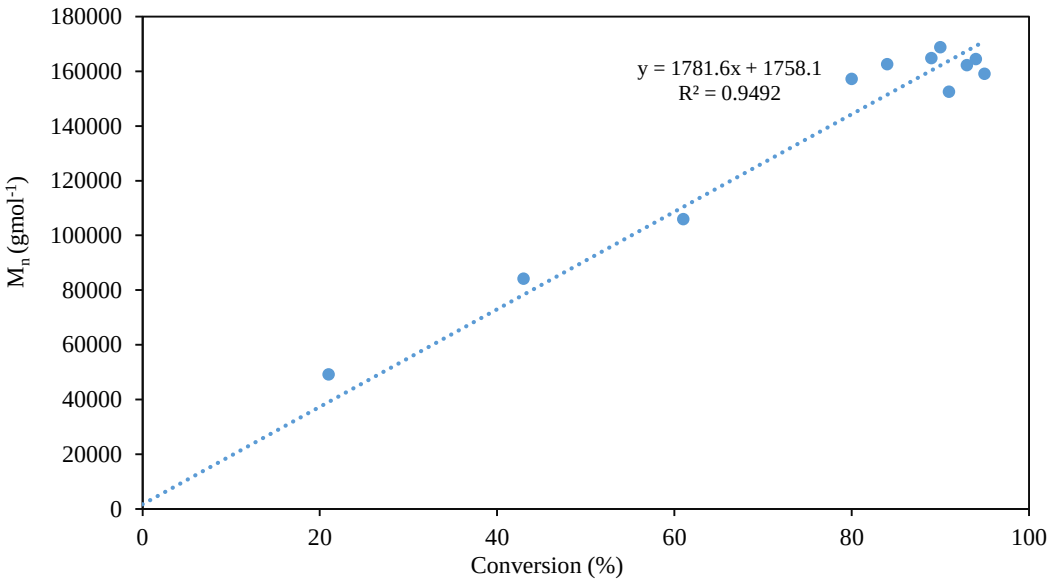

Figure S18. Plot of M_n vs conversion for the polymerisation of rac-lactide using [{L^{tBu}Nd(O*i*Pr)}$_2$] at 80 °C in toluene at a ratio of 1500:1 {[LA]:[Ln]}, [LA] = 0.69 M. Time samples taken via aliquots from a stirred solution.

Gel Permeation Chromatography Traces

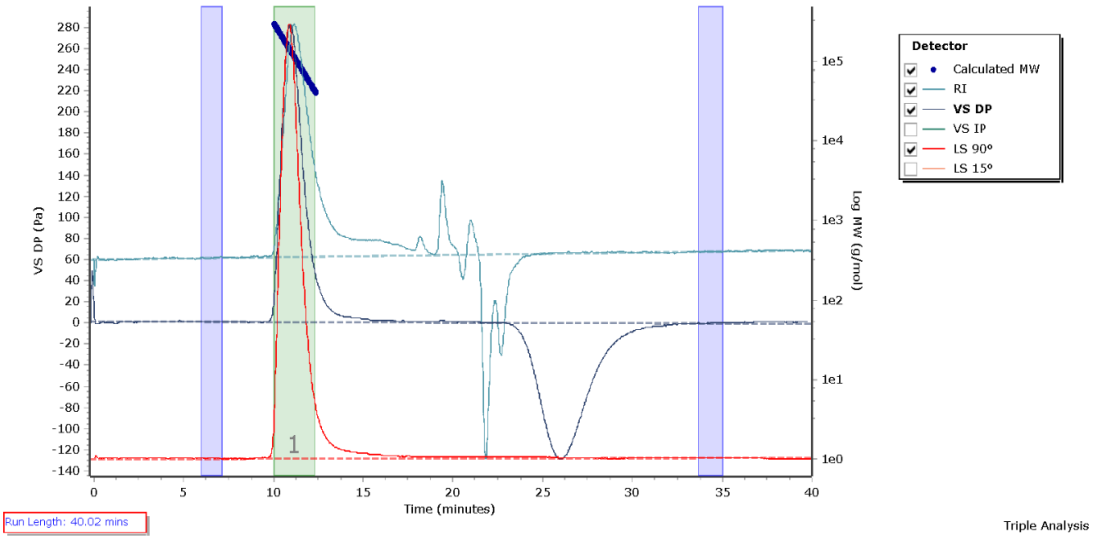

Figure S19. GPC trace of PLA initiated by [$L^{tBu}_2Sm_2$(O*i*Pr)(OH)] at ratios of 1000:1 {[LA]:[Ln]} at 25 °C in CH_2Cl_2 (Entry 7, Table S1). M_w^{GPC}(gmol^{-1}) = 140.3, M_n^{GPC}(kgmol^{-1}) = 92.3, $Đ$ = 1.51, M_n^{Theo}(kgmol^{-1}) = 136.9.

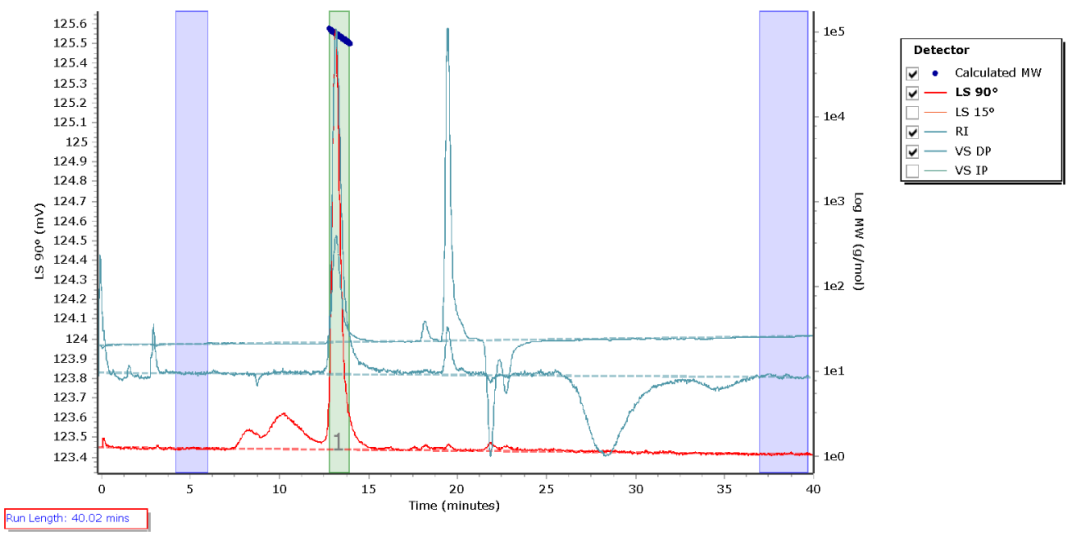

Figure S20. GPC trace of PLA initiated by [$L^{tBu}_2Yb_2$(O*i*Pr)(OH)] at ratios of 500:1 {[LA]:[Ln]} at 25 °C in CH_2Cl_2 (Entry 8, Table S1). M_w^{GPC}(gmol^{-1}) = 38.3, M_n^{GPC}(kgmol^{-1}) = 36.5, $Đ$ = 1.05, M_n^{Theo}(kgmol^{-1}) = 28.8.

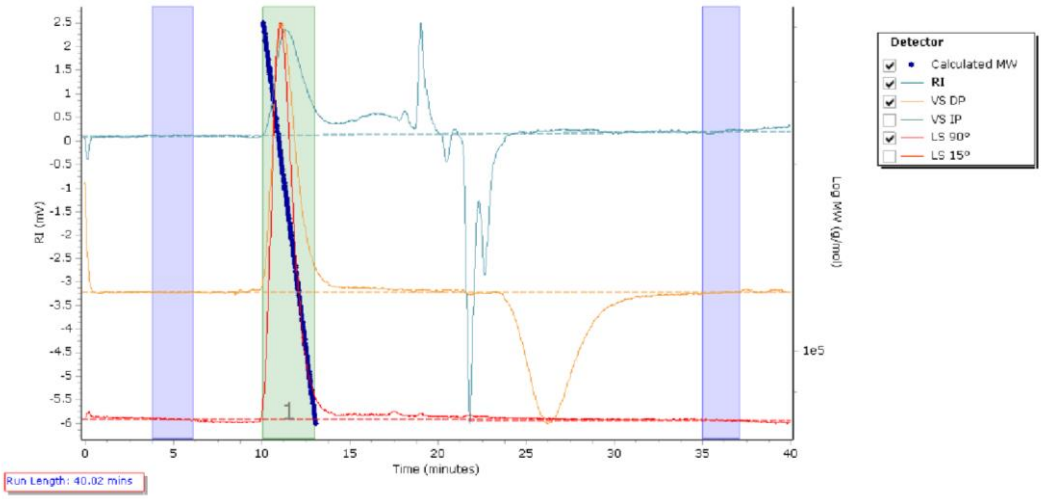

Figure S21. GPC trace of PLA initiated by [{L^{tBu}Nd(O*i*Pr)}$_2$] at ratios of 500:1 {[LA]:[Ln]} at 25 °C in CH_2Cl_2 (Entry 1, Table S1). M_w^{GPC}(gmol^{-1}) = 283.2, M_n^{GPC}(kgmol^{-1}) = 208.3, $Đ$ = 1.36, M_n^{Theo}(kgmol^{-1}) = 68.5.

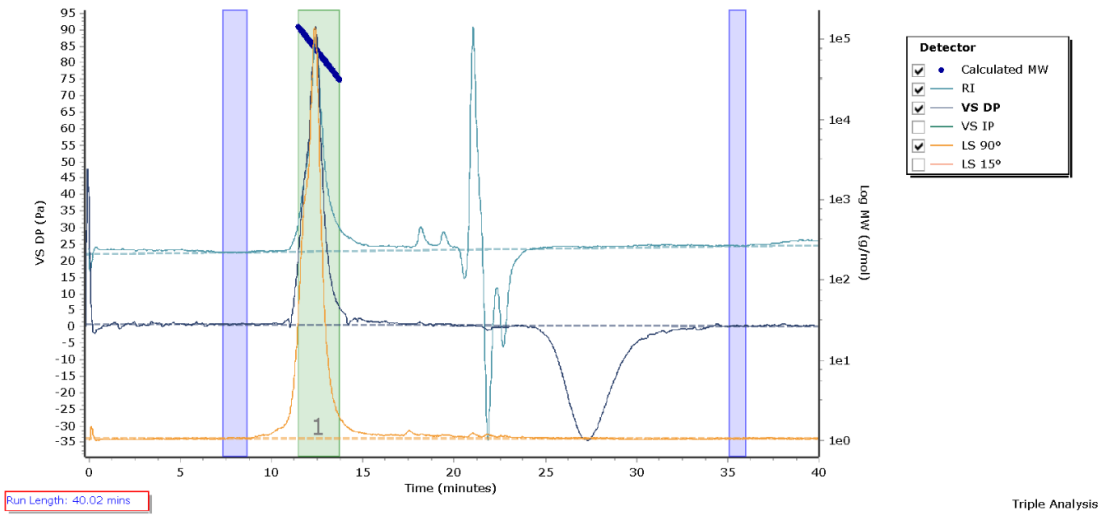

Figure S22. GPC trace of PLA initiated by [L$^{tBu}{}_2$Yb$_2$(O*i*Pr)(OH)] at ratios of 500:1 {[LA]:[Ln]} at 80 °C in toluene (Entry 9, Table S2). M_w^{GPC}(gmol^{-1}) = 76.6, M_n^{GPC}(kgmol^{-1}) = 69.0, $Đ$ = 1.11, M_n^{Theo}(kgmol^{-1}) = 68.5.

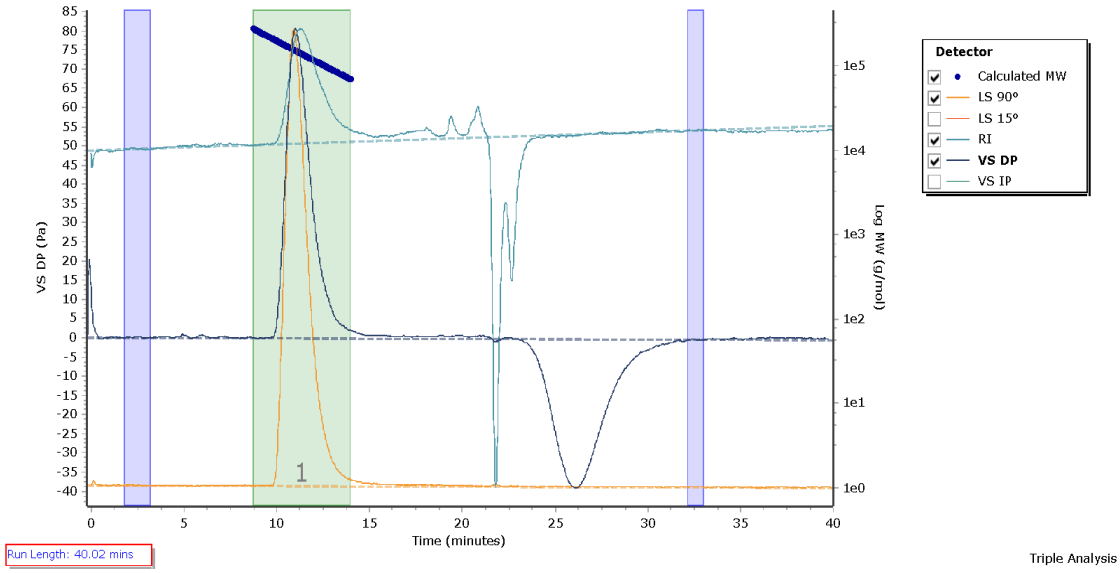

Figure S23. GPC trace of PLA initiated by [{L^{tBu}Nd(O*i*Pr)}$_2$] at ratios of 900:1 {[LA]:[Ln]} at 130 °C (Entry 1, Table S3). M_w^{GPC}(gmol^{-1}) = 128.2, M_n^{GPC}(kgmol^{-1}) = 122.1, $Đ$ = 1.05, M_n^{Theo}(kgmol^{-1}) = 123.1.

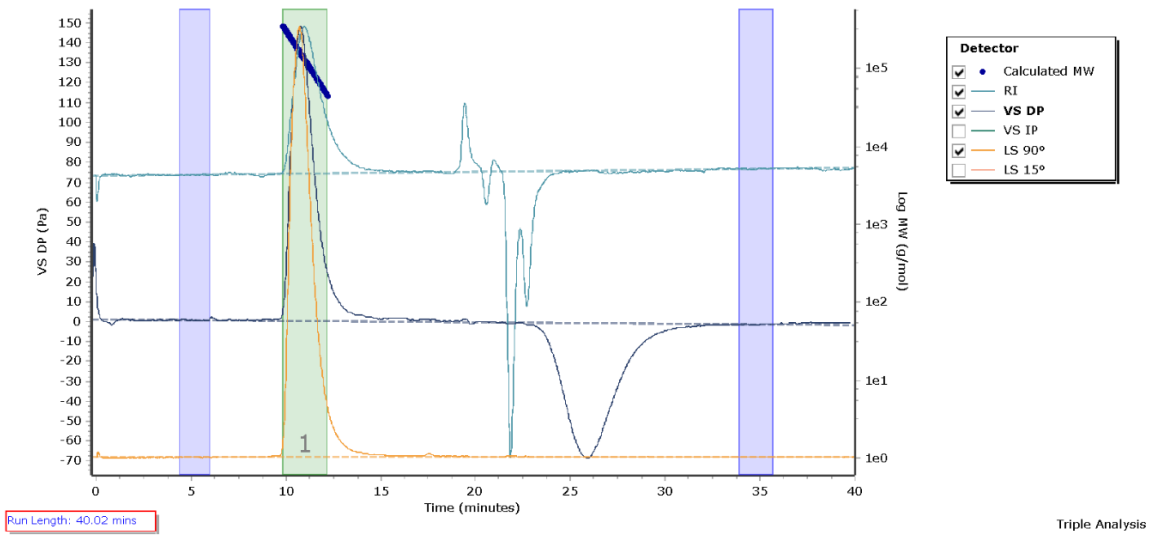

Figure S24. GPC trace of PLA initiated by [{L^{Me}Yb(O*i*Pr)}$_2$] at ratios of 900:1 {[LA]:[Ln]} at 130 °C (Entry 4, Table S3). M_w^{GPC}(gmol^{-1}) = 159.7, M_n^{GPC}(kgmol^{-1}) = 128.8, $Đ$ = 1.24, M_n^{Theo}(kgmol^{-1}) = 118.1.

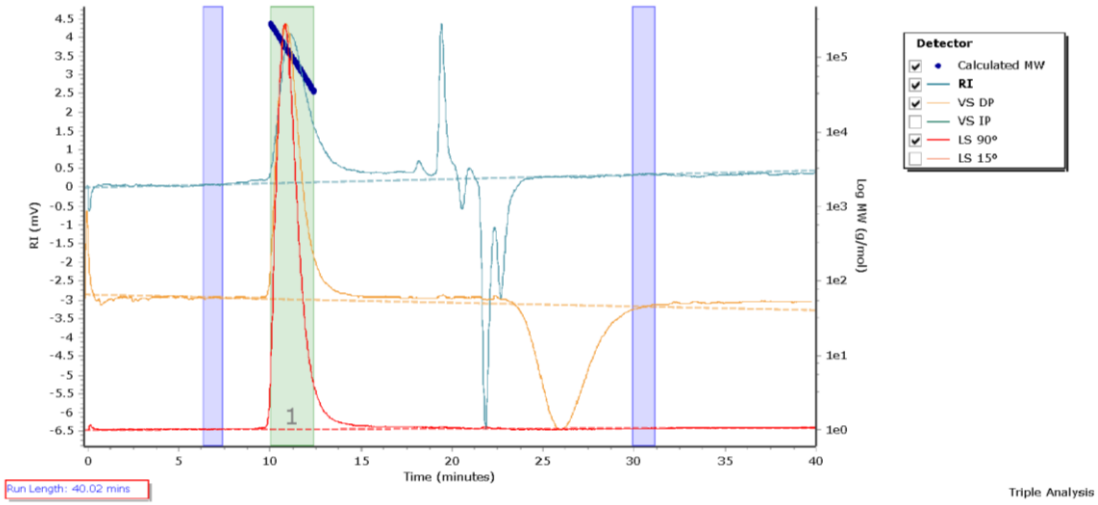

Figure S25. GPC trace of PLA initiated by [L$^{tBu}_2$Sm$_2$(O*i*Pr)(OH)] at ratios of 900:1 {[LA]:[Ln]} at 130 °C. (Entry 3, Table S3). M_w^{GPC}(gmol^{-1}) = 197.8, M_n^{GPC}(kgmol^{-1}) = 136.4, $Đ$ = 1.45, M_n^{Theo}(kgmol^{-1}) = 106.4.

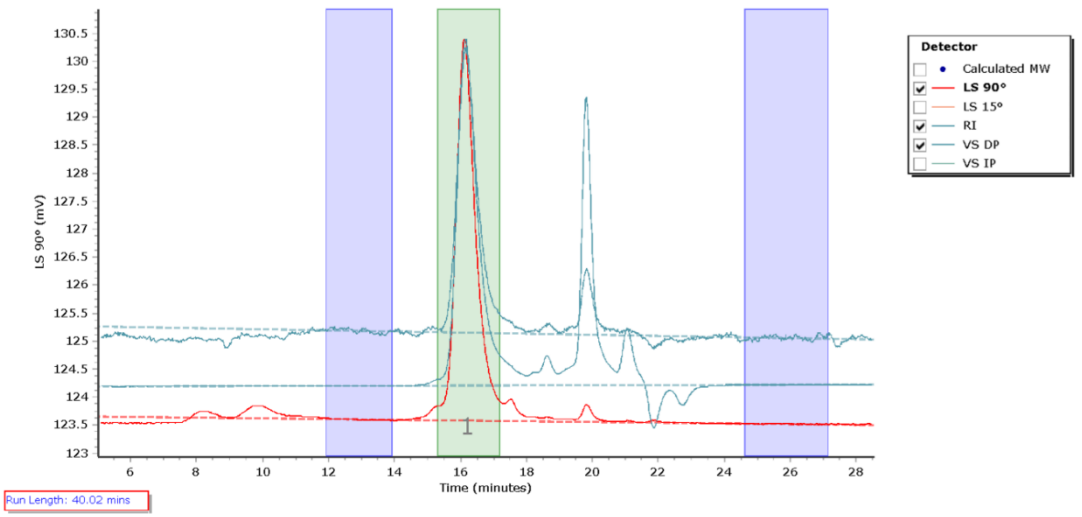

Figure S26. GPC trace of PLA initiated by [{L^{Me}Sm(O*i*Pr)}$_2$] at ratios of 20:1 {[LA]:[Ln]} in CDCl$_3$, 298 K, 5 hours, (Entry 4, Table 3). M_w^{GPC}(gmol^{-1}) = 2.9, M_n^{GPC}(kgmol^{-1}) = 2.8, $Đ$ = 1.02, M_n^{Theo}(kgmol^{-1}) = 2.6.

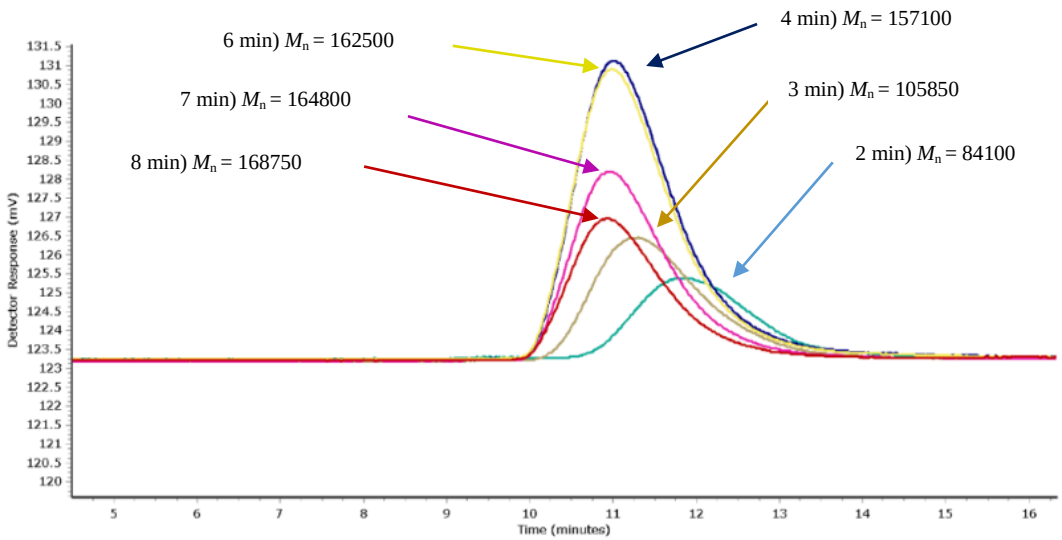

Figure S27. Stacked GPC traces of PLA initiated by [{L^{tBu}Nd(O*i*Pr)}$_2$] at ratios of 1500:1 {[LA]:[Ln]} at 80 °C in toluene. Time samples are taken from aliquots method. Stacked plots are taken from the raw LS 90° trace. M_n (gmol^{-1}), calculated from triple detection methods.

MALDI-ToF Analysis

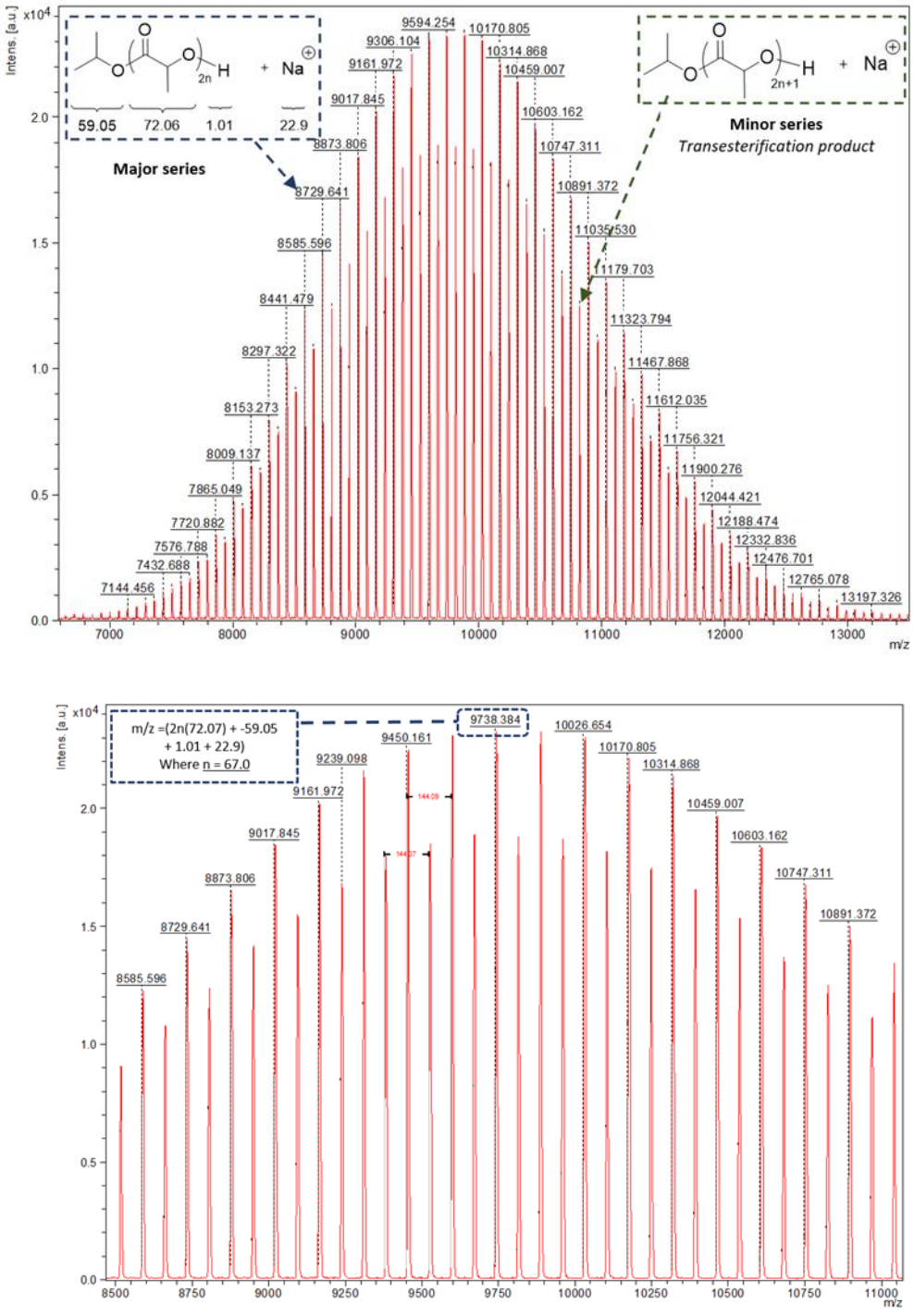

Figure S28. MALDI-ToF mass sprectra of polylactic acid from the polymerisation of *rac*-lactide with [{L^{Me}Sm(O*i*Pr)}$_2$] at ratios of 150:1 ([LA]:[Ln]) in CH_2Cl_2, 25°C (Entry 3, Table S1). Conversion = 40 %. Time = 2 hours. M_n^{GPC}(kgmol^{-1}) = 5.8, M_n^{Theo}(kgmol^{-1}) = 8.7. Linear polymer with O^{i}Pr + H end groups. The presence of a minor series of indicates a degree of transesterification is present.

Single Crystal X-Ray Diffraction Data

Table S4. Crystallographic data for solid state structures.

Compound reference	[{L^{Me}Yb(O*i*Pr)}$_2$]	[L$^{tBu}_2$Yb$_2$(O*i*Pr)(OH)]	[{L^{tBu}Nd(O*i*Pr)}$_2$]	[{L^{Me}Sm(O*i*Pr)}$_2$]	[{L^{tBu}Sm(OH)}$_2$]	[L$^{tBu}_2$Sm$_2$(O*i*Pr)(OH)]	[{L^{tBu}Sm(O*i*Pr)}$_2$]
Chemical formula	$C_{65}H_{82}N_4O_6Yb_2$	$C_{185}H_{286}N_8O_{12}Yb_4$	$C_{110}H_{162}N_4Nd_2O_6$	$C_{65}H_{90}N_4O_6Sm_2$	$C_{97}H_{142}N_4O_6Sm_2$	$C_{185}H_{286}N_8O_{12}Sm_4$	$C_{94}H_{158}N_4O_6Sm_2$
Formula Mass	1361.42	3506.36	1924.90	1324.10	1760.84	3415.60	1740.96
Crystal system	Monoclinic	Triclinic	Monoclinic	Monoclinic	Monoclinic	Triclinic	Monoclinic
a/Å	24.3739(4)	11.4225(10)	19.3846(5)	24.6223(9)	18.1468(2)	11.3821(4)	14.9466(2)
b/Å	11.55720(10)	20.2868(12)	24.2686(6)	11.6978(3)	21.0931(2)	20.7041(7)	15.2718(2)
c/Å	24.3550(4)	21.5670(17)	10.9610(3)	24.2817(9)	12.25180(10)	21.4578(8)	20.4709(2)
α/°	90	65.578(7)	90	90	90	66.212(3)	90
β/°	120.374(2)	77.839(7)	96.970(2)	119.614(5)	105.3320(10)	77.270(3)	92.9960(10)
γ/°	90	88.124(6)	90	90	90	87.858(3)	90
Unit cell volume/Å^3	5918.98(18)	4440.1(6)	5118.4(2)	6080.2(4)	4522.74(8)	4505.8(3)	4666.33(10)
Temperature/K	150(2)	150(2)	150(2)	150(2)	150(2)	150(2)	150(2)
Space group	*C*2/*c*	$P\bar{1}$	$P2_1/c$	*C*2/*c*	$P2_1/c$	$P\bar{1}$	$P2_1/c$
No. of formula units per unit cell, *Z*	4	1	2	4	2	1	2
No. of reflections measured	10339	35041	10771	50350	35230	45044	72176
No. of independent reflections	10339	16785	10771	8408	8982	23204	9343
R_{int}	-	0.0270	-	0.0278	0.0452	0.0255	0.0601
Final R_1 values ($I > 2\sigma(I)$)	0.0394	0.0268	0.0472	0.0262	0.0314	0.0323	0.0380
Final $wR(F^2)$ values ($I > 2\sigma(I)$)	0.1311	0.0622	0.1144	0.0529	0.0776	0.0636	0.0982
Final R_1 values (all data)	0.0438	0.0349	0.0665	0.0319	0.0370	0.0510	0.0421
Final $wR(F^2)$ values (all data)	0.1374	0.0658	0.1216	0.0551	0.0810	0.0711	0.1011

Bibliography

1 H. Kato, T. Saito, M. Nabeshima, K. Shimada and S. Kinugasa, *J. Magn. Reson.*, 2006, **180**, 266–273.

2 R. Evans, G. Dal Poggetto, M. Nilsson and G. A. Morris, *Anal. Chem.*, 2018, **90**, 3987–3994.

3 R. Evans, Z. Deng, A. K. Rogerson, A. S. McLachlan, J. J. Richards, M. Nilsson and G. A. Morris, *Angew. Chemie - Int. Ed.*, 2013, **52**, 3199–3202.

4 M. D. Jones, L. Brady, P. McKeown, A. Buchard, P. M. Schäfer, L. H. Thomas, M. F. Mahon, T. J. Woodman and J. P. Lowe, *Chem. Sci.*, 2015, **6**, 5034–5039.